ELSEVIER

Nuclear Instruments and Methods in Physics Research A 487 (2002) 136–141

NUCLEAR INSTRUMENTS & METHODS IN PHYSICS RESEARCH Section A

www.elsevier.com/locate/nima

Monte Carlo simulation of the response of a pixellated 3D photo-detector in silicon

E. Dubarić[a,b,*], H.-E. Nilsson[a], C. Fröjdh[a], B. Norlin[a]

[a] *Department of Information Technology and Media, Mid-Sweden University, Holmgatan 10, SE-851 70 Sundsvall, Sweden*
[b] *Solid State Electronics, Department of Microelectronics and Information Technology, Royal Institute of Technology (KTH), Electrum 229, SE-164 40 Kista, Sweden*

Abstract

The charge transport and X-ray photon absorption in three-dimensional (3D) X-ray pixel detectors have been studied using numerical simulations. The charge transport has been modelled using the drift-diffusion simulator MEDICI, while photon absorption has been studied using MCNP. The response of the entire pixel detector system in terms of charge sharing, line spread function and modulation transfer function, has been simulated using a system level Monte Carlo simulation approach. A major part of the study is devoted to the effect of charge sharing on the energy resolution in 3D-pixel detectors. The 3D configuration was found to suppress charge sharing much better than conventional planar detectors.

PACS: 07.05.Tp; 07.07.Df; 07.85.Fv; 85.60.Gz; 87.59.−e

Keywords: Monte Carlo simulation; Three-dimensional; X-ray; Detector; Silicon; Charge sharing

1. Introduction

Improved process techniques, like laser drilling and dry etching that make it possible to drill deep holes and to dope and fill them, have made a new silicon detector approach very interesting. The suggested detector structure, as shown in Fig. 1(a), which was first suggested by Parker et al. in Ref. [1], has the potential to solve the shortcomings of the current silicon X-ray detectors. Another structure that has been suggested is to fill the holes with a scintillating material in order to improve the light detection efficiency and the spatial resolution [2]. The short distance between the charge collecting electrodes leads to shorter drift times, higher electric fields, and smaller operating voltages. Initial simulations of the detector structure in Fig. 1(b) suggest that an applied bias of ~ 1 V is needed to fully deplete the device. There are other possible detectors layout, like the hexagonal structure, but the one in Fig. 1(b) has a simple matrix format very well suited for direct conversion to standard digital image formats.

In this work, we have used a Monte Carlo approach on the system level to investigate the response for a 3D X-ray pixel detector in silicon in terms of charge sharing, line spread function (LSF) and modulation transfer function (MTF).

*Corresponding author. Tel.: +46-6014-8879; fax: +46-6014-8830.

E-mail address: ervin.dubaric@ite.mh.se (E. Dubarić).

0168-9002/02/$ - see front matter
PII: S0168-9002(02)00957-9

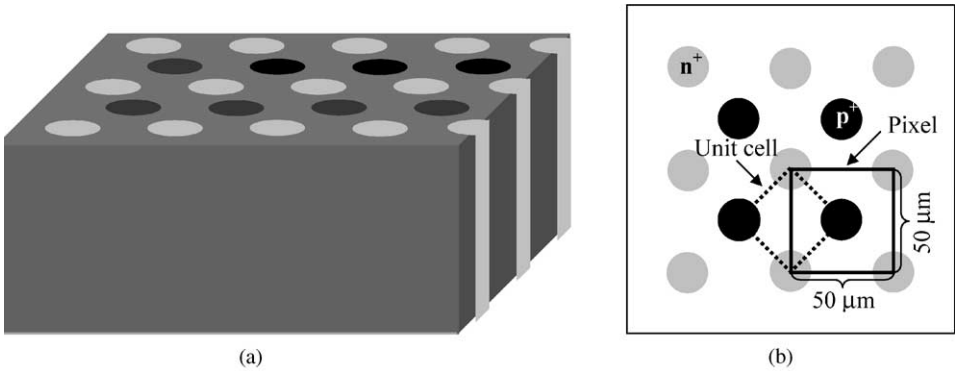

Fig. 1. (a) Three-dimensional X-ray pixel detector structure, (b) unit cell and simulated structure.

2. Charge sharing

Constraints within medical and dental X-ray imaging, such as patient dose reduction and higher resolution, demand detector structures with better spatial resolution. One possible solution to meet these constraints is smaller pixel dimensions. A major drawback with shrinking pixel sizes is that the charge sharing between two adjacent pixels becomes more pronounced. The charge sharing has a large impact on the energy resolution in a photon counting system, since the pulse height will not correspond to the energy of the photon. In the energy spectrum this effect results in a redistribution of the signal towards lower energies. Other drawbacks with smaller pixel size are lower signal-to-noise ratio and smaller dynamic range. A methodology to determine an optimal pixel size is presented in Ref. [3].

There is a conceptual difference between charge sharing in 2D and 3D X-ray detectors. In a 2D detector, the X-ray photon induced charge cloud will diffuse during its drift towards the charge collecting electrode, i.e., the drift does not suppress the charge sharing, whereas in a 3D detector the charge sharing is suppressed by the drift, see Fig. 2. This means that the charge sharing should be less severe in the latter detector type, which consequently should have better performance.

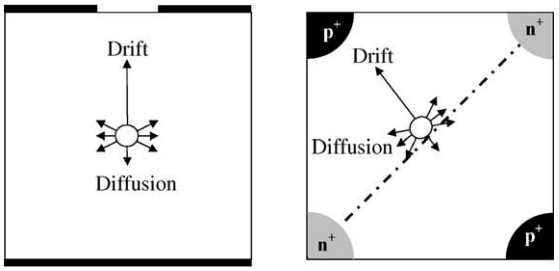

Fig. 2. Principal difference between charge sharing in: (left) a 2D pixel detector, and (right) a 3D pixel detector.

2.1. Charge sharing study using MEDICI

In order to make an initial study of the charge sharing in the suggested 3D structure, simulations of the transient of single photon absorption were performed using the commercial 2D-semiconductor device simulator MEDICI from Avant! Corp. [4]. The simulator solves numerically and self-consistently Poisson's equation in two dimensions, electron and hole continuity equations, and electron and hole current equations. Recombination mechanisms implemented in the simulator include Shockley–Read–Hall (SRH), Auger and band-to-band statistics.

In Fig. 3, the simulated unit cell (see Fig. 1) is presented. The stars indicate the simulated points of photon absorption in the detector. Due to the symmetry of the device, only half of it was

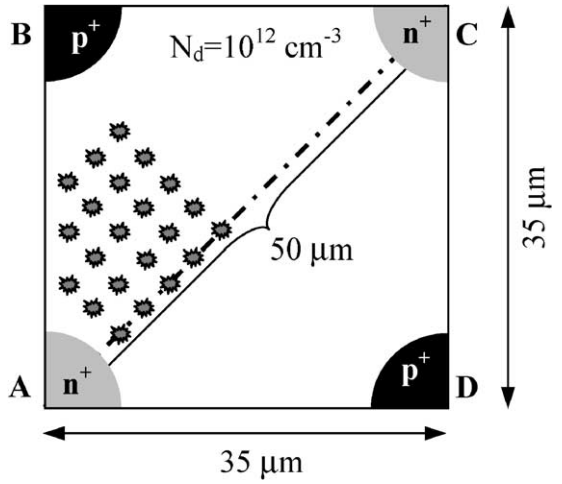

Fig. 3. Simulated unit cell. The stars indicate the location of a single photon absorption.

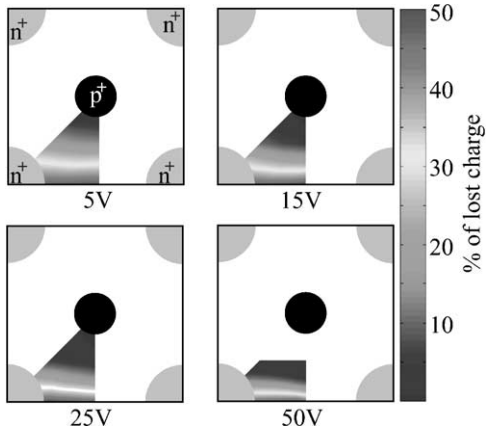

Fig. 4. Simulated percentage of charge sharing at different bias levels.

simulated. In the simulations we have assumed a point-like mono-energetic X-ray source of 30 keV. The number of electron–hole pairs created at this energy level is approximately 8310, corresponding to a peak carrier concentration of $5 \times 10^{16}\,\mathrm{cm}^{-3}$. Default silicon material parameters and standard drift-diffusion transport parameter values in MEDICI were used. It should be noted that 3D plasma effects in the charge cloud have been neglected. A full 3D drift-diffusion simulation is needed in order to take these effects into account. However, for the drift distances and the electric field strength considered in this work, this approximation is of minor importance.

In Fig. 4, the percentage of collected charge for different biases at contact **B** is presented. As can be seen, the region sensitive to charge sharing is decreased by a factor of two when the applied voltage is increased by a factor of 10. The main reason for this can be understood by considering the relation between drift time and diffusion. The diffusion equation and its solution can be written as [5]

$$\frac{\partial \Delta n}{\partial t} = D_n \frac{\partial^2 \Delta n}{\partial x^2} \tag{1}$$

$$\Delta n = \left[\frac{\Delta n_0}{2\sqrt{\pi D_n t}}\right] \mathrm{e}^{-(x^2/4D_n t)} \tag{2}$$

where Δn is the excess carrier concentration, D_n is the diffusion constant and Δn_0 is the peak excess concentration at $t = 0$. Using this approximation it is possible to write the charge spread as

$$\Delta x = 4\sqrt{D_n t} \tag{3}$$

where Δx is the full width at 37% of the top value. This simple expression shows that there is a square root relation between charge spread and drift time. The symmetry of the 3D detector is such that the drift path a charge cloud experiences will be independent of the bias voltage. The electric field along the drift path will change and thus the drift time. An increase in the voltage bias with a factor of 10 will decrease the drift time with approximately the same factor. The corresponding decrease in charge spread will thus be $1/\sqrt{10} = 0.3$. Charge spread is directly related to the size of the charge sharing regions in the detector, which explains the simulation results.

2.2. System level Monte Carlo simulation of the imaging performance

The charge collection in a 3D detector is different from charge collection in 2D detectors. In the 2D detector, the charge cloud is spherical and the charge collection at the detector surface can be described using a radial distribution. However, in a 3D detector the charge-collecting electrode is a cylinder, and as the charge cloud

moves closer to the collecting electrode, the cloud will be reduced in size and transformed into a non-spherical shape. At the system level the details regarding the shape and size of the charge cloud is not important, as long as the overall charge sharing effects close to the pixel boundaries are accurately modelled. An advantage with the 3D detector is that the charge sharing is not dependent on the depth of the absorption event as in the 2D detector. This indicates that it is possible to use a system level Monte Carlo model developed for 2D detectors to estimate the effect of charge sharing on the system performance, if a proper radial charge distribution is used. The choice of radial charge distribution should be such that it reproduces the charge sharing characteristics of the 3D-pixel detector.

The system level Monte Carlo simulation is performed using the following algorithm:

For each simulated photon:

1. Select photon energy according to the distribution function of the X-ray source.
2. Select the position of the X-ray absorption randomly according to the 3D-energy deposition distribution function obtained using MCNP [6].
3. Assigned charges to the pixel electrodes using the fixed radial charge distribution.

A more detailed description of the system level Monte Carlo model is presented in Ref. [7].

In order to verify that our model provides reasonable results, we have applied our model to the same 3D-detector structure as used in the experiments presented by Kenney et al. [8]. They used a ^{55}Fe X-ray source to study the energy resolution of a 3D-strip detector with a strip spacing of 200 μm. The measured full-width-at-half-maximum (FWHM) was 618 eV. In Fig. 5, the energy spectrum obtained by simulation of the same detector structure using a narrow peak X-ray source (FWHM value of 590 eV) is presented. The energy spectrum obtained is similar to what has been observed experimentally, which shows that the simulation model provides reasonable accuracy.

As a measure of the image resolution of an X-ray pixel detector, the LSF and the MTF are commonly used [9]. An experimental way to get the MTF is based on the X-ray illumination of a slit, which is tilted with respect to the detector array and placed on top of it. The LSF is then obtained by plotting the intensity in each pixel as a function of the distance l between the centre of the

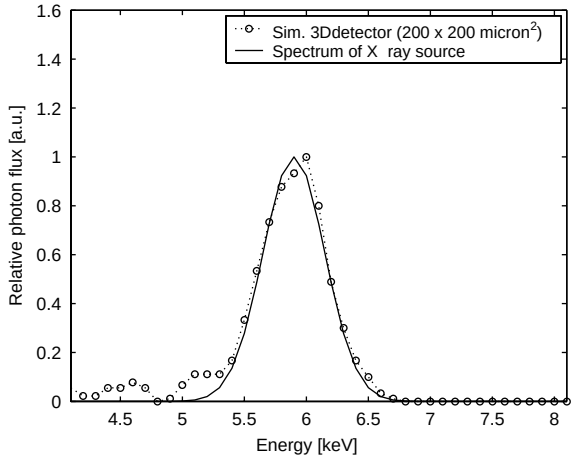

Fig. 5. Simulated energy spectrum for a 200 μm strip detector illuminated with a narrow-peak X-ray source similar to the ^{55}Fe source used in Ref. [8].

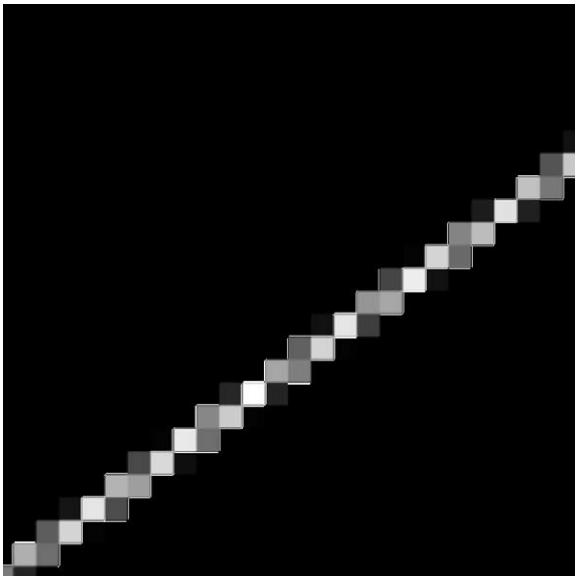

Fig. 6. The simulated image of a 10 μm wide slit on top of a 3D detector with a pixel size of $50 \times 50\,\mu m^2$.

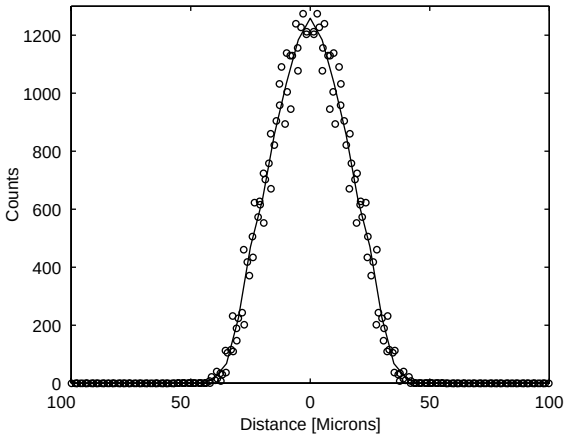

Fig. 7. Extracted line spread function (LSF) from the image in Fig. 6.

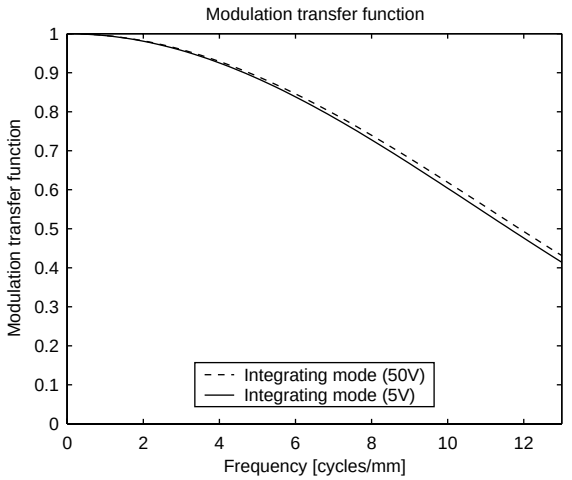

Fig. 8. Modulation transfer function (MTF) for a 3D detector with a pixel size of $50 \times 50\,\mu m^2$ at 5 and 50 V bias.

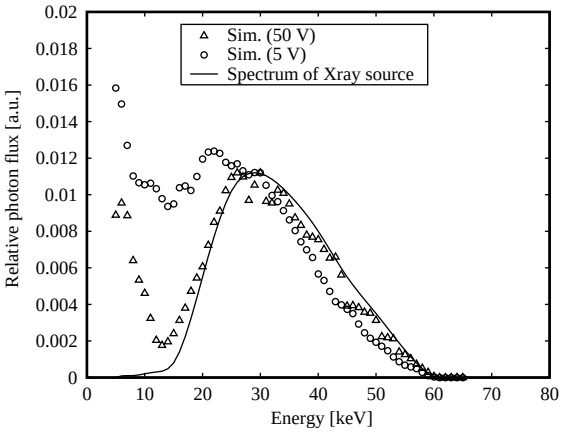

Fig. 9. Simulated energy spectrum for a 3D detector with a pixel size of $50 \times 50\,\mu m^2$ at 5 and 50 V bias.

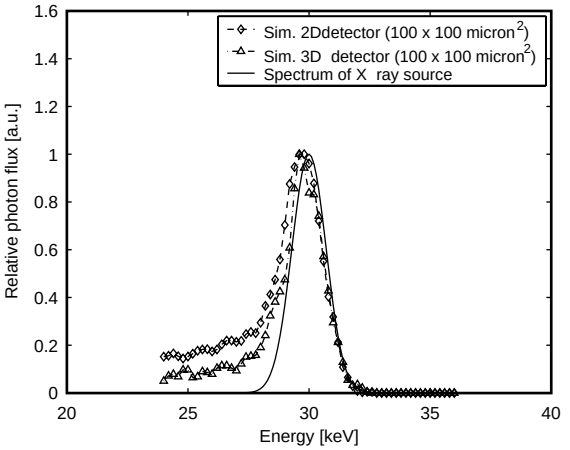

Fig. 10. Comparison of simulated energy spectrum for 2D and 3D detectors with a pixel size of $100 \times 100\,\mu m^2$.

pixel and the position of the slit; the MTF is the Fourier transform of the LSF. Fig. 6 presents the simulated image of a 10 μm slit on top of a 25×25 pixel detector array while the corresponding LSF is presented in Fig. 7.

In Fig. 8, the MTF for the bias conditions of 5 and 50 V is presented. According to the MEDICI simulations the charge sharing at 50 V should be lower than 5 V. The effect of this difference can be seen in Fig. 9, where the simulated energy spectrum from a flood exposure of a dental X-ray source is presented. There is a large difference between the 5 and 50 V bias. The large difference in the energy spectrum is not visible in the spatial resolution (see Fig. 8). The main reason for this can be found in the way the spatial resolution is extracted. The spatial resolution is first of all limited by the pixel size. As long as the pixel size is much larger than the charge spread, the spatial resolution will be limited by the pixel size. A more detailed discussion regarding the effect of charge sharing on the spatial resolution can be found in Ref. [7].

In Fig. 10, the simulated energy spectrum for both 2D and 3D configurations are compared. The X-ray source used has a narrow peak at 30 keV with a FWHM of 1.66 keV. The simulated 3D detector had a bias of 10 V, which is needed in order to fully deplete the $100 \times 100\,\mu m^2$ pixel detector. The energy resolution of the 3D detecor at this bias is significantly better than the resolution of the 2D detector. The difference will be even larger at a bias voltage of 50 V.

3. Conclusions

In this paper, we have studied the charge sharing effects in a 3D X-ray pixel detector for dental applications by simulations using a drift-diffusion transport model. The charge sharing at the pixel boundary has been studied as a function of different bias voltages. This study has been used to set up a system level Monte Carlo simulation model in order to model the imaging properties of 3D-detector systems. Both spatial and energy resolution have been studied. A comparison with the experimental energy resolution obtained for 200 μm slit detector in Ref. [8] shows that the model can reproduce the experimental result, which indicates that the model has a reasonable accuracy. The simulated energy spectrum for a 3D detector with a pixel size of $50 \times 50\,\mu m^2$ and illuminated by a standard dental X-ray source, show that under these conditions a high bias voltage is needed in order to suppress the distortion due to charge sharing. A detailed comparison of the charge sharing in lateral detectors and 3D detectors show that the charge sharing is significantly lower in the 3D detector. The charge sharing in 3D detectors is mainly reduced due to a higher electric field, a shorter drift path and localisation of the charge to one pixel due to the potential well structure in 3D detectors.

Acknowledgements

The Mid-Sweden University in Sundsvall, Sweden, and the KK-Foundation, Sweden, are gratefully acknowledged for their financial support.

References

[1] S.I. Parker, C.J. Kenney, J. Segal, Nucl. Instr. and Meth. A 395 (1997) 328.
[2] P. Kleimann, J. Linnros, C. Fröjdh, C.S. Petersson, Nucl. Instr. and Meth. A 460 (2001) 15.
[3] Ting Chen, et al., Proc. SPIE 3965 (2000) 1.
[4] Avant! Corporation, MEDICI, Two-dimensional Device Simulation Program, Version 4.1, User Manual, TCAD Business Unit, Freemont, CA, USA, 1998.
[5] B.G. Streetman, Solid State Electronic Devices, 4th Edition, 1995, p. 123.
[6] Los Alamos Monte Carlo Group, MCNP-4B General Monte Carlo N-Particle Transport Code, Los Alamos National Laboratories Report LA-12625-M, 1997.
[7] H-E. Nilsson, E. Dubaric, M. Hjelm, K. Bertilsson, Nucl. Instr. and Meth. A 487 (2002), 151, these proceedings.
[8] C.J. Kenney, et al., IEEE Trans. Nucl. Sci. NS-48 (2001) 189.
[9] A. Workman, D.S. Brettle, Dentomaxillofacial Radiol. 26 (1997) 139.